The EMBO Journal Vol. 19 No. 19 pp. 5123–5134, 2000

CD95 (APO-1/Fas) linkage to the actin cytoskeleton through ezrin in human T lymphocytes: a novel regulatory mechanism of the CD95 apoptotic pathway

Stefania Parlato[1], Anna Maria Giammarioli[2], Mariantonia Logozzi[1], Francesco Lozupone[3], Paola Matarrese[2], Francesca Luciani[3], Mario Falchi[2], Walter Malorni[2] and Stefano Fais[3,4]

Laboratories of [1]Virology, [2]Ultrastructures and [3]Immunology, Istituto Superiore di Sanità Viale Regina Elena 299, 00161 Rome, Italy

[4]Corresponding author
e-mail: Fais@iss.it

S.Parlato and A.M.Giammarioli contributed equally to this work

CD95 (APO-1/Fas) is a member of the tumor necrosis factor receptor family, which can trigger apoptosis in a variety of cell types. However, little is known of the mechanisms underlying cell susceptibility to CD95-mediated apoptosis. Here we show that human T cells that are susceptible to CD95-mediated apoptosis, exhibit a constitutive polarized morphology, and that CD95 colocalizes with ezrin at the site of cellular polarization. In fact, CD95 co-immunoprecipitates with ezrin exclusively in lymphoblastoid CD4+ T cells and primary long-term activated T lymphocytes, which are prone to CD95-mediated apoptosis, but not in short-term activated T lymphocytes, which are refractory to the same stimuli, even expressing equal levels of CD95 on the cell membrane. Pre-treatment with ezrin antisense oligonucleotides specifically protected from the CD95-mediated apoptosis. Moreover, we show that the actin cytoskeleton integrity is essential for this function. These findings strongly suggest that the CD95 cell membrane polarization, through an ezrin-mediated association with the actin cytoskeleton, is a key intracellular mechanism in rendering human T lymphocytes susceptible to the CD95-mediated apoptosis.

Keywords: apoptosis/CD95 Fas/cytoskeleton/ezrin/polarization

Introduction

Between the major programmed cell death (PCD) pathways, CD95 (APO-1/Fas)-mediated apoptosis seems one of the most involved in both the physiological control of cell proliferation and in the pathogenesis of viral, autoimmune and neoplastic diseases (Linch *et al*., 1995; Giordano *et al*., 1997; Nagata, 1997; Apoptosis, special section, 1998; Peter and Krammer, 1998). Particularly, the CD95 interaction with its ligand (FasL) plays a crucial role in homeostasis and self-tolerance of lymphocytes in both humans and mice (Nagata and Suda, 1995). However, despite abundant surface expression, cells may be either susceptible or refractory to CD95-mediated PCD (Klas *et al*., 1993; Suda *et al*., 1997). In fact, susceptibility to the CD95-mediated apoptosis may not be merely due to the surface expression of the CD95 antigen, in that lymphocytes equally expressing CD95 on the membrane are differently triggerable to PCD (Klas *et al*., 1993; Alderson *et al*., 1995; Brunner *et al*., 1995). Intracellular mechanisms involved in the positive or negative regulation of the CD95-signaling pathway have been described (Tschopp *et al*., 1998). However, cellular susceptibility to CD95-mediated PCD remains an unresolved issue and the search for novel mechanisms is necessary. Asymmetric organization of the plasma membrane and cytosolic organelles is fundamental for a variety of cells, including pro- and eukaryotic cells (Nelson, 1992). The degree to which cells polarize is characterized by their ability to create and maintain morphologically and biochemically distinct plasma membrane domains. The prototype of stable polarized membrane domains are the apical and basolateral surfaces of simple epithelial cells. However, T lymphocytes continuously change their shape and polarization, rapidly orienting their cytoskeletal components during interaction with antigen presenting cells (Stowers *et al*., 1995) or following chemokine stimulation (del Pozo *et al*., 1996). The ability of a cell to polarize is directly related to the membrane/cytoskeleton association (Drubin and Nelson, 1996), and the interactions between plasma membrane and cytoskeleton play an essential role in various cellular functions (Luna and Hitt, 1992; Kusumi and Sako, 1996; Dransfield *et al*., 1997; Tsukita *et al*., 1997; Defacque *et al*., 2000). Among the proteins that have been suggested to link the actin cytoskeleton to the plasma membrane are members of the ezrin family (ezrin, radixin, moesin and merlin) (Bretscher, 1999; Mangeat *et al*., 1999). The ERM proteins (ezrin, radixin and moesin) are found in the microvilli, filopodia, membrane ruffles and cell-to-cell contact sites where they colocalize with actin and have been shown to connect various cell-surface proteins to the actin cytoskeleton (Tsukita *et al*., 1994; Kusumi and Sako, 1996; Serrador *et al*., 1997, 1998; Heiska *et al*., 1998; Yonemura *et al*., 1998). On the basis of these considerations, we investigated cells susceptible to CD95-mediated apoptosis, such as human lymphoblastoid T cells and activated primary lymphocytes: (i) the level of polarization; (ii) the cellular expression, distribution and molecular association of CD95 and ezrin, radixin and moesin (ERM); and (iii) the effects of ERM antisense oligonucleotides or actin-perturbing agents on CD95-mediated apoptosis.

Results

CD95/ezrin co-localize in human T lymphocytes

We have observed by time-lapse cinematography (TLC) that human lymphoblastoid CD4+ T cells, highly susceptible to CD95-mediated apoptosis (CEM cells), con-

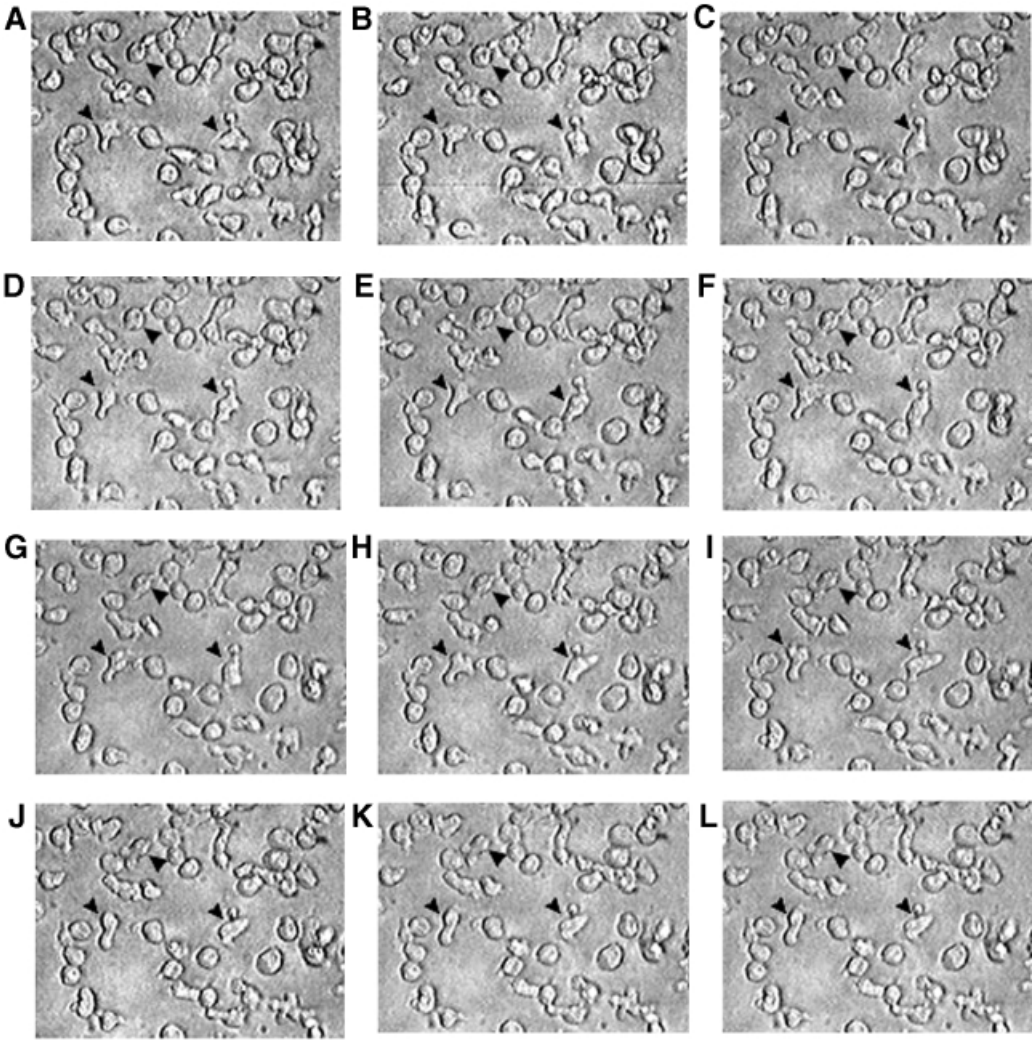

Fig. 1. Time lapse video microscopy of CEM cells. Picture sequence (**A**–**L**) was obtained from TLC of CEM cells cultured on poly-L-lysine-covered glass chamber slides. The sequence shows morphological changes occurring in living cells within 1 h. A micrograph every 5 min is shown. These represent the same field at the same magnification (400× original magnification) and display a number of cells forming or retracting their uropodial protrusions. Arrowheads indicate representative cells forming uropodes.

tinuously underwent giant uropod formation during culture (Figure 1). Uropods can be defined as long (at least one third of the whole cell body) and large bulbs transiently protruding from the cell surface. Unlike 'blebs', which generally appear as small and permanent blisters typical of cells undergoing apoptosis, uropods are considered as a marker of cell viability and serve as a sort of cell–cell interaction 'device'. Figure 1 shows sequential micrographs of CEM cells forming or retracting uropods under culture conditions. The data obtained by scanning electron microscopy (SEM) were highly consistent with those shown with TLC. In fact, CEM cells appeared as highly polarized cells with the whole cytoplasm unidirectionally oriented into giant uropods, either adhering (Figure 2A) or non-adhering (Figure 2B) to the substrate. We calculated that up to 30% of CEM cells presented clear uropod formations and that the vast majority of the cells showed pre-uropoidal structures, such as pseudopods. Thus, immunocytochemistry, immunofluorescence and intensified charge-coupled device video microscopy (IVM) were used to assess the CD95 distribution on CEM cells. The results showed that CD95 was constitutively polarized on CEM cells, as shown by both immunofluorescence (Figure 2C) and immunocytochemical staining (Figure 2D). The same results were obtained with another $CD4^+$ T cell line (Hut78 cells) (Figure 2E and F). Notably, up to 90% of the cells presented CD95 polarization on uropods and/or pseudopods. To verify the specificity of CD95 polarization, we analyzed both CEM and Hut78 cells, by immunofluorescence and immunocytochemistry, the distribution of tumor necrosis factor reptor1 (TNFR1), belonging to the same family of receptors. The results showed that TNFR1, consistently with flow cytometric analysis, was weakly expressed on CEM cells (data not shown). Hut78 cells expressed TNFR1 that was uniformly distributed on the cell membrane without any clear feature of polarization (Figure 2G and H). It is known that the polarized state of a cell is determined and maintained by the actin cytoskeleton, and that membrane proteins that commonly polarize in the cells are frequently associated to the actin cytoskeleton through the ERM family proteins (Kusumi

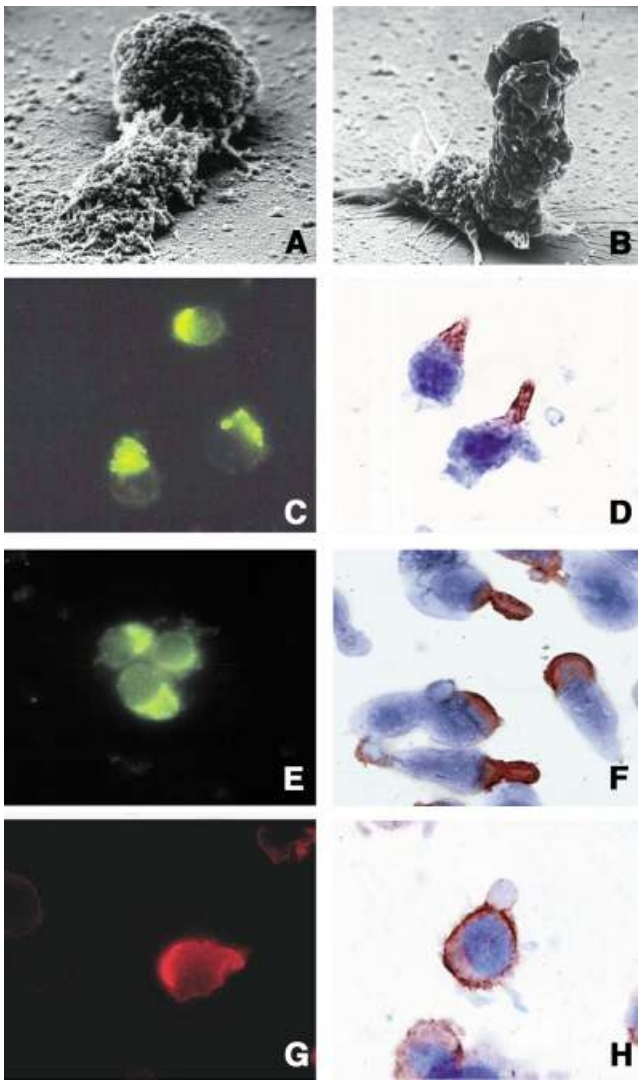

Fig. 2. Uropod formation and CD95 polarization in CEM cells. SEM analysis of CEM cells adhering on polylysine-covered glass coverslips and forming giant uropodes characterized by a large blister body, which either remain attached to the substrate (**A**) or behave as a long ruffling edge (>2-fold of the cell body) (**B**). Magnification, ×35 000. Both intensified charge-coupled device video microscopy (IVM) (magnification, ×1000) and immunocytochemistry (magnification ×1500–2500) clearly show polarization of CD95 (APO-1/Fas) in CEM (**C** and **D**) and Hut78 (**E** and **F**) cells. IVM (magnification ×1500) (**G**) and immunocytochemistry (**H**) (magnification ×2500) clearly show the unpolarized distribution of tumor necrosis factor receptor (TNFR) in Hut78 cells.

and Sako, 1996). Therefore, we preliminarily assessed by RT–PCR the expression of the ERM transcripts in both CEM cells as compared with human primary T lymphocytes. The results showed that ezrin and moesin mRNAs were fully expressed by both CEM cells and primary lymphocytes, either resting or activated, while radixin transcripts were undetectable in these cells (Figure 3A), confirming a previous report (Shcherbina *et al*., 1999). These results excluded the possibility that radixin might be involved in the CD95 linkage to the actin cytoskeleton. Thus, we analyzed the ezrin and moesin protein expression and distribution in CEM cells. The results showed that the pattern of ezrin polarization was very similar to that of CD95 in the vast majority of CEM cells (85–90%), as shown by both immunofluorescence (Figure 3B) and immunocytochemistry (Figure 3C), while moesin, even highly expressed in these cells (Figure 3D and E), did not exhibit a cellular polarization comparable to those shown for CD95 and ezrin, being virtually absent in CEM cells uropods. Double staining experiments clearly showed colocalization of CD95 and ezrin using either immunofluorescence (Figure 3F) or immunocytochemistry (Figure 3G), while moesin was not shown to colocalize with CD95 protein (Figure 3H). Thus, we have explored the sensitivity for anti-CD95-mediated induction of apoptosis in human primary $CD4^+$ T cells activated *in vitro*. Consistent with a previous paper (Klas *et al*., 1993), short-term (day 1) and long-term (day 6) activated $CD4^+$ T cells, although expressing comparable amounts of CD95 on the cell membrane showed marked differences in sensitivity to CD95-mediated apoptosis (Figure 4A). In fact, virtually all the day 1-activated $CD4^+$ T cells expressed marked levels of both activation markers and CD95 but did not undergo apoptosis following the anti-CD95 monoclonal antibody (mAb) treatment, while the vast majority of day 6-activated $CD4^+$ T cells were highly sensible to the mAb treatment (Figure 4A). Notably, both in day 1- and day 6-activated $CD4^+$ T cells, virtually all the $CD95^+$ CD4 T cells were $CD45RO^+$, confirming that the membrane expression of CD95 is highly related to the memory phenotype in these cells (Miyawaki *et al*., 1992; De Maria *et al*., 1996). Thus, consistently with a previous study (Klas *et al*., 1993), we showed that the differential susceptibility of activated $CD4^+$ T cells to the CD95-mediated apoptosis was independent of the cell membrane expression of CD95. Thus, we explored by IVM the ezrin/CD95 co-localization in human primary lymphocytes. The results showed that, consistent with CEM cells, ezrin and CD95 were highly polarized and co-localized in day 6-activated lymphocytes, while day 1-activated lymphocytes did not exhibit any polarization event (Figure 4B). Notably, in the vast majority (90–95%) of both CEM cells and activated primary lymphocytes, CD95 and ezrin co-localized in uropods or pseudopods.

These results showed that: (i) human lymphoid cells susceptible to the CD95-mediated apoptosis frequently presented a clear polarized shape; (ii) in these cells CD95 polarized on uropods or pseudopods; (iii) susceptibility of human primary $CD4^+$ T cells to the CD95-mediated apoptosis did not depend on the CD95 expression on the cell membrane; and (iv) the co-localization of CD95 with ezrin was a typical pathway of human $CD4^+$ T cells highly susceptible to the CD95-mediated apoptosis.

Notably, polarization of a membrane protein and its co-localization with a protein of the ERM family are the first and more important features suggesting a possible molecular association to the actin cytoskeleton (Nelson *et al*., 1992; del Pozo *et al*., 1996; Kusumi and Sako, 1996; Tsukita *et al*., 1997).

Actin cytoskeleton involvement in susceptibility to CD95-mediated apoptosis

To explore whether the association of CD95 with the actin cytoskeleton was involved in the CD95-dependent apoptosis, we investigated the effects of cytoskeletal-

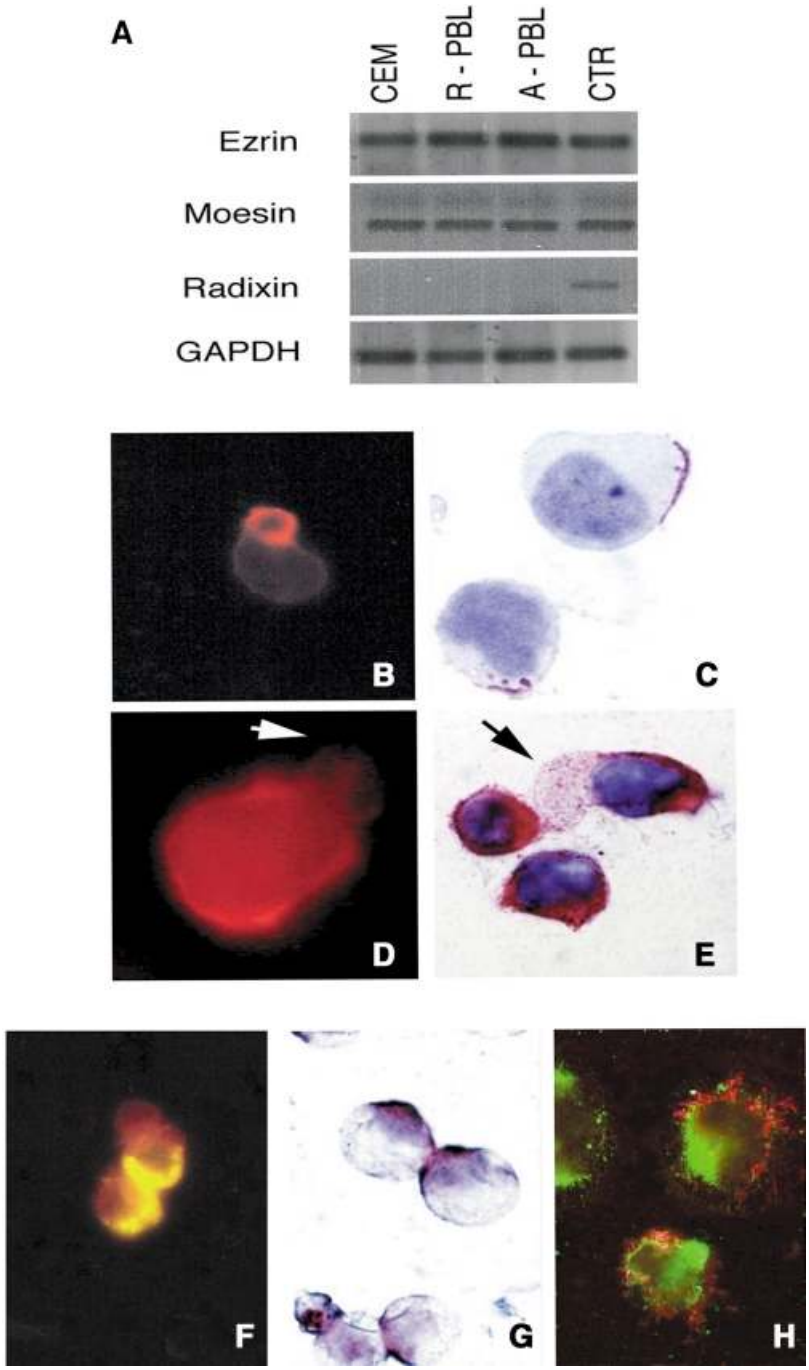

Fig. 3. ERM expression and distribution in CEM cells. (**A**) RT–PCR analysis of ezrin, moesin and radixin mRNAs in CEM cells, resting and day 6-activated peripheral blood lymphocytes (PBL). Human monocytes were used as positive control for ezrin and moesin, and HepG2 cells as positive control for radixin. (**B**) and (**C**) IVM (magnification ×1000) and immunocytochemistry (ICC) (magnification ×2500), respectively, for ezrin that is clearly detectable on uropod formations of CEM cells. (**D**) and (**E**) show IVM (magnification ×1500) and ICC (magnification ×2500), respectively, for moesin that, even though markedly expressed, was virtually undetectable in CEM cell uropods. Arrows in (D) and (E) indicate moesin-negative uropods. Double staining experiments showed a polarized co-localization for CD95 and ezrin in CEM cells, as detected by yellow staining in immunofluorescence (due to red, TRITC, and green, FITC, overlapping) (**F**) (magnification 1000×) and by brown staining in immunocytochemistry (overlapping of red, PAP/AEC, and blue, APAAP/NBT) (**G**) (magnification ×1500). (**H**) A double staining for CD95 (green, FITC) and moesin (red, TRITC). Notably, the CD95 staining (green) is localized in uropods or pseudopods, while the moesin staining is widely distributed (magnification ×1500).

perturbating agents on the apoptosis induced by a CD95-triggering mAb in cultures of CEM cells. Thus, we treated CEM cells with non-cytotoxic doses of cytochalasin D (CD), analyzing its effects on cell morphology and CD95 membrane distribution. The results showed that CD treatment induced a loss of cell polarity (Figure 5A) compared with untreated cells (Figure 5B), and an unpolarized redistribution of CD95 on the membrane of CEM cells (Figure 5C). Thus, we challenged CEM cells with a CD95-triggering mAb and other apoptotic stimuli (a physical agent, UVB, and a chemical agent, staurosporin), with or without pre-treatment with CD. As shown in

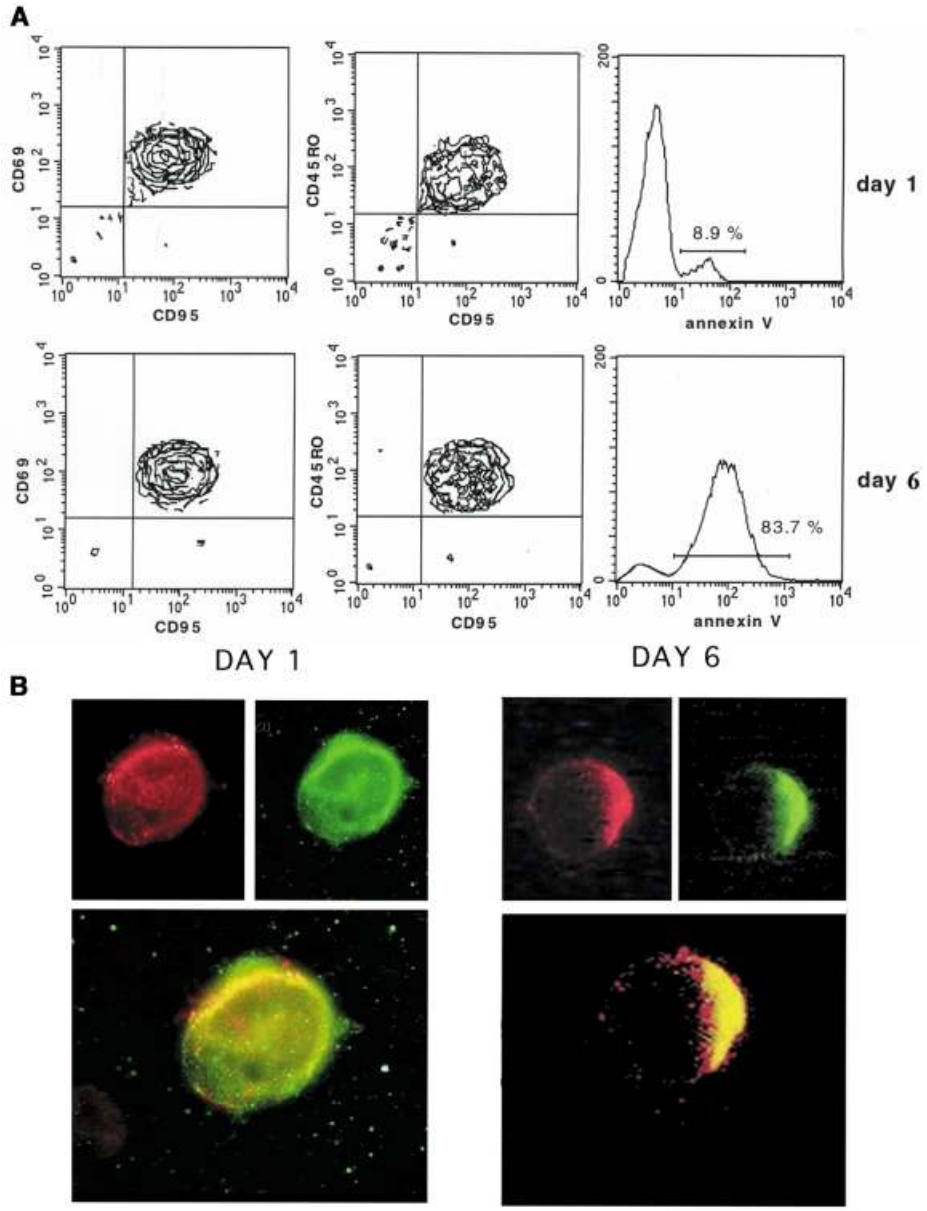

Fig. 4. CD95 expression, susceptibility to apoptosis and CD95/ezrin co-localization in activated human primary T lymphocytes. (**A**) CD95 membrane expression and apoptosis were analyzed in electronically gated $CD4^+$ by three-color immunofluorescence and FACS analysis in day 1- (upper panels) and day 6- (lower panels) activated human primary lymphocytes (PBL). Left panels are the $CD95^+/CD69^+$ $CD4^+$ PBL; central panels are the $CD95^+/CD45RO^+$ $CD4^+$ lymphocytes; right panels are the apoptotic cells (FITC–annexin V+) CD4+ PBL after triggering with an anti-CD95 mAb (see Materials and methods). The results are representative of four experiments. (**B**) CD95 (green, FITC)/ezrin (red, TRITC) localization in day 1- (left panel) and day 6- (right panel) activated human primary T lymphocytes. In the upper and lower panels the single and double stainings are shown, respectively. Note the co-localization in day 6-activated lymphocytes, as revealed by the yellow staining (IVM) (magnification ×1000).

Figure 5D, the results, obtained by both static (DNA labeling dye) and flow cytometric (propidium iodide) analyses, clearly demonstrated that CD significantly protected CEM cells from the CD95-induced apoptosis, while inhibition of actin polymerization did not affect staurosporin- nor UVB-induced apoptosis. The TNFα stimulation (at the doses not inducing oxidative stress) (Larrick and Wright, 1990; Mehlen *et al*., 1995) did not induce detectable apoptosis both in CEM and Hut78 cells with or without CD treatment (data not shown). Accordingly, SEM analyses showed that CD pre-treatment was highly effective in preventing the typical actin cytoskeleton-dependent surface alterations of apoptosis (i.e. collapsed and peduncolated membrane blebs) induced by the CD95 triggering, but not in preventing the other apoptotic stimuli (data not shown). Notably, CEM cells treated with the anti-CD95 mAb, UVB or staurosporin in the absence of CD exhibited the actin-related morphological features of apoptosis maintaining the prominent uropoidal bodies (data not shown).

CD95/ezrin association

To explore further the cellular distribution of CD95 in human $CD4^+$ T cells highly susceptible to CD95-mediated apoptosis, CEM cells extracts were fractionated into cytosolic, cytoskeletal and membrane fractions, and

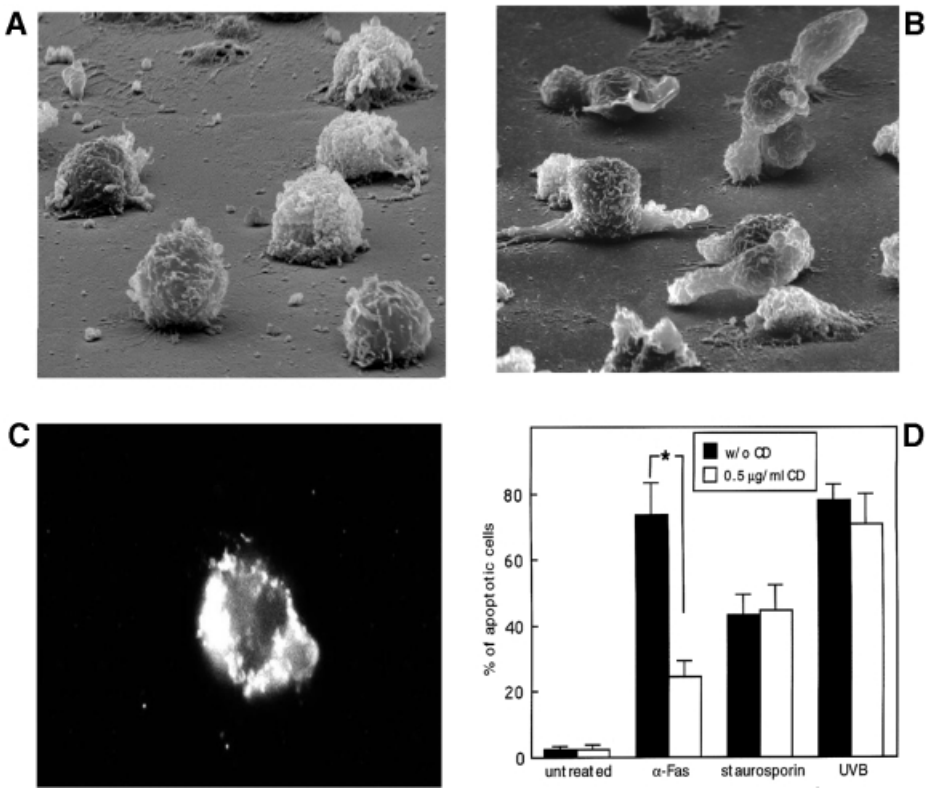

Fig. 5. Cytochalasin D effects on CEM cell morphology, CD95 distribution and CD95-mediated apoptosis. SEM analysis of cytochalasin D (CD)-treated (**A**) and untreated (**B**) CEM cells. Note the disappearance of uropoidal shape with preservation of microvillar structures, small pseudopodia and ruffle spreading in CD-treated cells (magnification ×35 000). (**C**) Immunofluorescence analysis of CD95 distribution on CEM cells following cytochalasin D (CD) pre-treatment. Note the scattered distribution of CD95 protein throughout the cell cytoplasm (magnification ×1000). (**D**) Effects of CD pre-treatment on CD95-mediated apoptosis compared with the apoptosis induced by UVB, or staurosporin. Histograms represent mean ± SD of five different experiments. *Student's *t*-test, $P < 0.001$.

analyzed by western blotting, compared with the whole-cell extracts. The results showed that CD95 and ezrin were comparably detectable in the membrane and cytoskeletal fractions (Figure 6A), while CD95 was undetectable in the cytosol. Figure 6A includes control experiments showing that CD4 was detected predominantly in the membrane fraction, actin in the cytoskeletal fraction and caspase-3 exclusively in the cytosolic fraction. Thus, we performed reciprocal experiments blotting the ezrin mAb on CD95 immunoprecipitates and the anti-CD95 mAb on ezrin immunoprecipitates in CEM cell lysates, to investigate the CD95 association to ezrin, and, as a consequence, to the actin cytoskeleton. These experiments were performed using Laemmli buffer to avoid the usual migration of the IgG heavy chains around 50 kDa, thus covering the CD95-specific band (see Material and methods). In fact, Figure 6B showed that the specific CD95 band was clearly detectable in both ezrin and CD95 immunoprecipitates (left panel), while virtually all the IgGs migrated to the top of the filter (without the usual dissociation between light and heavy chains) both in the immunoprecipitates and in control experiments using antibodies in lysate buffer. Figure 6B also includes the results of ezrin blotting in either CD95 or ezrin immunoprecipitates, showing that ezrin was consistently detectable in the CD95 immunoprecipitates (right panel). Figure 6B shows that the CD95 bands detectable in the ezrin immunoprecipitates was roughly comparable to the CD95 bands obtained by western blotting in whole lysates (left panel), while the ezrin band in the CD95 immunoprecipitates was clearly smaller than the ezrin band in whole lysates (right panel), suggesting that the majority of CD95 was associated to ezrin, while only one-third of ezrin was associated to CD95. Moesin and CD95 did not appear to immunoprecipitate reciprocally in CEM cells (Figure 6B, left panel). To confirm this finding further under physiological conditions we investigated the CD95/ezrin association in day 1- and day 6-activated human primary purified T lymphocytes, namely in cells with comparable amounts of CD95 on the cell membrane but with different susceptibilities to CD95-mediated apoptosis (see Figure 4). The results showed that, consistent with the human lymphoblastoid $CD4^+$, the anti-CD95 antibody reacted with the ezrin immunoprecipitates, and the anti-ezrin antibody reacted with the CD95 immunoprecipitates obtained from cytoskeletal plus membrane fractions of day 6-activated T lymphocytes (Figure 6C, right panel), while day 1-activated T lymphocytes did not show CD95/ezrin molecular association in both conditions (Figure 6C, left panel). Figure 6C also shows the lack of association between CD95 and moesin, in that moesin was undetectable in the CD95 immunoprecipitates in both day 1- and day 6-activated primary T lymphocytes. This set of results strongly suggested a specific interaction between CD95 and ezrin in human $CD4^+$ T cells susceptible to CD95-mediated apoptosis.

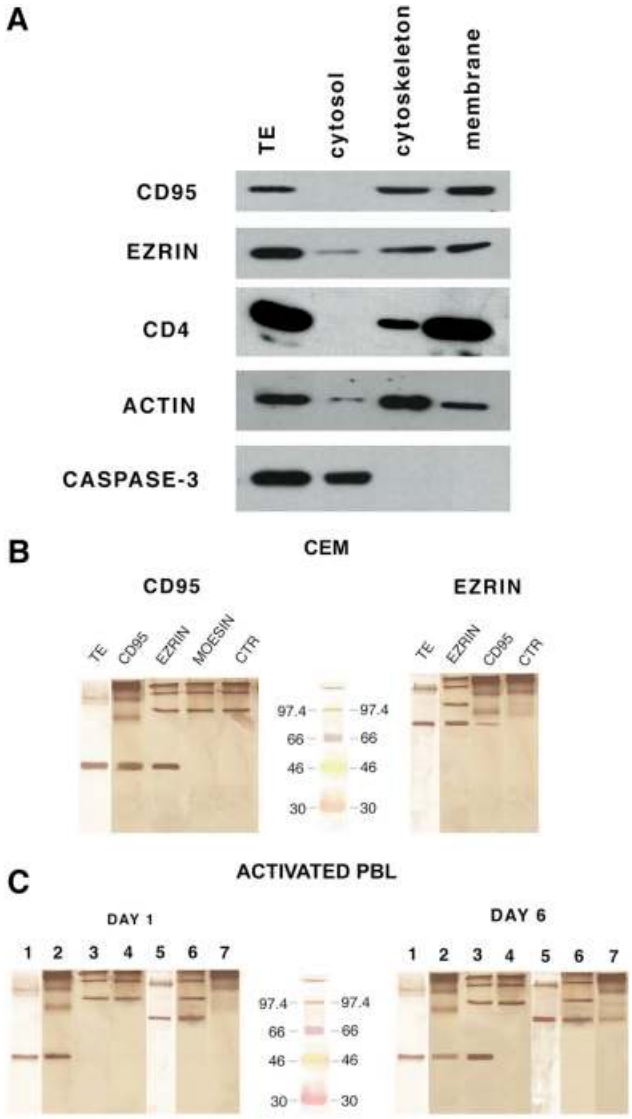

Fig. 6. CD95 association to ezrin. (**A**) Western blotting for CD95, ezrin, CD4, actin and caspase-3 expression in total extracts (TE) of CEM cells and in subcellular fractions of CEM cells. The specific molecular weights are 45, 80, 59, 42 and 32, respectively. (**B**) Western blotting for CD95 (left panel) and ezrin (right panel) in various immunoprecipitates or total extracts (TE) of CEM cells, as indicated in the figure. The figure was obtained using the DAKO EnVision™ system, HRP and DAB as chromogen (DAKO, Denmark). Note migration of IgG (without the usual dissociation between the light and heavy chains) on the top of the filter (due to the absence of β-mercaptoethanol in the Laemmli buffer). Controls using the antibodies in lysate buffer are also included (anti-CD95, left panel; anti-ezrin, right panel). Prestained standards not containing β-mercaptoethanol (Rainbow ™ colored protein molecular weight markers, Amersham UK) are included (central lane). (**C**) Western blotting (WB) with mAbs to CD95 or ezrin in total extract or various immunoprecipitates from cell lysates of day 1- (left panel) and day 6- (right panel) activated human lymphocytes. Lane 1, WB for CD95 on total extracts (TE); lane 2, WB for CD95 on CD95 immunoprecipitates; lane 3, WB for CD95 on ezrin immunoprecipitates; lane 4, WB for CD95 on moesin immunoprecipitates; lane 5, WB for ezrin on TE; lane 6, WB for ezrin on ezrin immunoprecipitates; lane 7, WB for ezrin on CD95 immunoprecipitates. Note the presence of ezrin in CD95 immunoprecipitates and CD95 in ezrin immunoprecipitates exclusively in day 6-activated PBL. Prestained standards not containing β-mercaptoethanol (Rainbow™ colored protein molecular weight markers, Amersham UK) are included (central lane).

The role of ezrin in CD95-mediated apoptosis

The data on CD95/ezrin co-localization and co-immunoprecipitation in human T cells susceptible to CD95-mediated apoptosis encouraged us to perform experiments aimed at evaluating the specific role of ezrin in CD95-mediated apoptosis. Thus, we treated CEM cells with antisense phosphorothioate oligonucleotides (PONs) complementary to internal sequences of the coding regions of human ezrin or moesin. The results firstly showed that treatment of CEM cells with both ezrin and moesin antisense PONs significantly inhibited the expression of ezrin as well as moesin proteins, respectively, as assessed by western blot analysis (Figure 7A). Using the same experimental conditions, we challenged CEM cells with the anti-CD95-triggering mAb with or without pre-treatment with PONs. The results analyzed by flow cytometry showed that the ezrin antisense PONs significantly inhibited the CD95-mediated apoptosis exclusively (Δ = –53.3%, P <0.001), while pre-treatment with the sense PONs or moesin antisense PONs did not show any significant effect compared with the controls (Figure 6B). In particular, Figure 7B shows that pre-treatment with the ezrin antisense PONs markedly decreased the percentage of cells undergoing both early (annexin V single-positive, lower right quadrant) and late (PI/annexin V double-positive, upper right quadrant) apoptosis as compared with the cells treated with the moesin antisense PONs. The cells pre-treated with the sense PONs were shown to behave as the untreated cells (PI/annexin V double-positive, upper right quadrants). Moreover, SEM, immunofluorescence and immunocytochemical analyses clearly showed that ezrin antisense PON treatment markedly inhibited microvilli and uropod formation, as well as CD95 distribution in treated cells (Figure 7C), while both ezrin sense PONs (Figure 7D) and moesin PONs (data not shown) did not apparently affect either morphology or CD95 distribution in CEM cells. These results strongly supported a specific role of ezrin in CD95-mediated apoptosis. In fact, moesin antisense PONs did not affect the cell susceptibility to CD95 triggering, suggesting distinct and specialized functions of ezrin and moesin in lymphocytes, as proposed in a recent study (Shcherbina *et al*., 1999).

Discussion

These results strongly suggest that susceptibility to CD95-mediated apoptosis in human T lymphocytes depends on the polarization of CD95 due to its association to the actin cytoskeleton through ezrin. It is thus conceivable that association of CD95 with the actin cytoskeleton may represent a major intracellular regulatory mechanism of CD95-mediated apoptosis in human $CD4^+$ T lymphocytes. In particular, it is possible that cytoskeleton-driven polarization of CD95 (APO-1/Fas) may facilitate CD95 clustering, rendering $CD4^+$ T cells susceptible to CD95-mediated apoptosis. Much evidence suggests that the interactions between the plasma membrane and the actin cytoskeleton are involved in many diverse functions of eukaryotic cells, including development and control of cell morphology and polarity, adhesion of a cell to extracellular matrix and cell-to-cell adhesion, membrane stability and membrane domain organization (Luna and Hitt, 1992; Drubin and Nelson, 1996). However, some

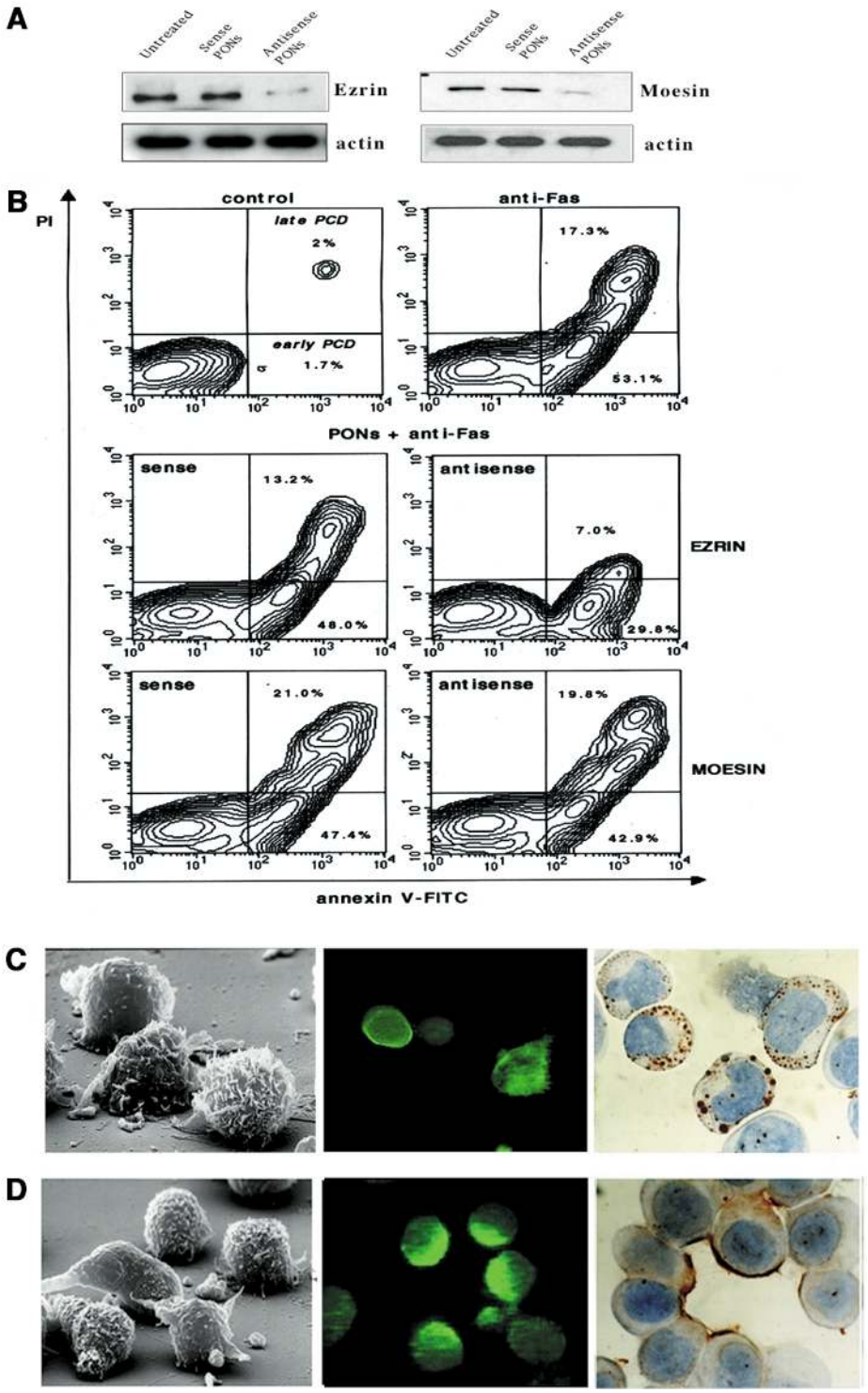

Fig. 7. Effects of phosphorothioate oligonucleotides (PONs) on CD95-mediated apoptosis. (**A**) Western blotting with mAbs to human ezrin and moesin in CEM cells lysates following sense or antisense PONs treatment or without treatment. Actin levels in the relative lysates are shown. (**B**) Flow cytometric analysis of CEM cells after double staining procedure with annexin V–FITC/PI performed on living cells. As specified in the control panel (upper left), in the upper right quadrants (annexin V–FITC/PI positive) and in the lower right quadrants (annexin V single positive) of all the panels are represented the cells in the early or late apoptosis, respectively. CEM cells were left untreated (upper left), treated with the anti-CD95 triggering mAb (upper right), treated with the anti-CD95 triggering mAb after pre-treatment with ezrin PONs (central panels) or moesin PONs (lower panels). SEM (left panel) and CD95 distribution, as detected by immunofluorescence (central panel) and immunocytochemistry (right panel), in CEM cells treated with ezrin antisense (**C**) or sense (**D**) PONs.

evidence strongly suggests that membrane-to-ERM family proteins interaction occurs indirectly through PDZ domain-containing ezrin-binding molecules (Kusumi and Sako, 1996; Cao *et al.*, 1999). Evidence has shown that ezrin can exist in a dormant and activated state, and that activation induces membrane–cytoskeletal association

(Kusumi and Sako, 1996). Of interest, long-term activated T lymphocytes are highly susceptible to CD95-mediated apoptosis, while short-term activated T lymphocytes are completely resistant to the apoptosis induced by the anti-CD95 mAb, despite the equal expression of CD95 on the cell membrane (Klas *et al*., 1993). Here we have shown that exclusively long-term activation of human peripheral T lymphocytes results in CD95–ezrin association and polarized co-localization. This strongly suggests that the CD95–ezrin–actin linkage is a crucial event in the homeostatic regulation of the immune response. Interestingly, polarization can occur in lymphocytes following: (i) chemokine stimulation (del Pozo *et al*., 1996); (ii) contact of helper T cells with antigen-presenting cells (APC) (Geiger *et al*., 1982; Kupfer *et al*., 1986, 1994); (iii) unidirectional budding of human immunodeficiency virus (HIV) during cell-to-cell infection (Fais *et al*, 1995). Our data strongly suggest that during the development of these phenomena, CD95 (APO-1/Fas) may be directed towards the T cell uropod, rendering the cell particularly susceptible to CD95-mediated apoptosis.

In recent years, the number of membrane proteins that have been shown to link to the actin cytoskeleton in human lymphoid and epithelial cells has grown impressively (Tsukita *et al*., 1994; Serrador *et al*., 1997, 1998; Yonemura *et al*., 1998; Bretscher, 1999). This linkage is frequently associated with the acquisition of a uropod-driven polarized shape, following adherence or cytokine stimulation in both lymphocytes and monocytes (Fais *et al*., 1994, 1997; del Pozo *et al*., 1997). Notably, uropods and cell-to-cell adhesion sites form and disappear continuously in cells observed in culture, suggesting that the cellular distribution of the cytoskeleton-associated membrane molecules may change over time. In fact, microfilament-perturbating agents such as cytochalasin D can disrupt actin microfilament organization and, as a consequence, cytoplasmic trafficking of molecules and various intracellular signaling pathways (e.g. integrin-mediated signaling via tyrosine kinase) (Clarke and Brugge, 1995; Maniotis *et al*., 1997; Yamada and Geiger, 1997). Our findings on CD95 (APO-1/Fas) association to the actin cytoskeleton through ezrin, support further the hypothesis that cytoskeletal components serve as a matrix, which regulates the efficiency of interactions between cell-surface-expressed transmembrane receptors and various catalytic and non-catalytic molecules of the signal transduction cascade. Notably, we have studied cells in which the CD95 pathway is by far the preferential apoptotic mechanism (Linch *et al*., 1995). However, we cannot exclude the possibility that other proteins belonging to the TNF receptor family may be linked directly to the actin cytoskeleton or that the well known intracellular cross-talk between the major proteins of this family (i.e. CD95 and TNFR) (Wallach *et al*., 1999) may be influenced by the linkage of one of these receptors to the actin cytoskeleton.

In conclusion, we have provided evidence that linkage of CD95 (APO-1/Fas) to the actin cytoskeleton through ezrin is a key factor in rendering human T lymphocytes, susceptible to CD95-mediated apoptosis. The possibility of interfering with the linkage between ERM proteins and CD95 should provide a novel tool to modulate the CD95-mediated apoptotic pathway in lymphocytes.

Materials and methods

Videomicroscopy

TLC was obtained using a phase contrast Nikon inverted microscope equipped with a Zeiss CCD camera and a JVC time lapse videotape recorder. Unfixed living CEM cells seeded on 0.1% poly-L-lysine-covered glass chamber slides at a density of 50 000 cells/ml at 40× magnification have been studied. Films were recorded under standard culture conditions (5% CO_2 humid atmosphere at 37°C). Uropod formation was clearly detected by decreasing tape speed by at least 360 times (to obtain a quick-time movie after an overnight recording).

SEM analysis

CEM cells were fixed with 2.5% (v/v) glutaraldehyde in 0.1% cacodylate buffer (pH 7.4) and processed as described previously (Malorni *et al*., 1993a). Samples were then examined with a Cambridge 360 SEM.

Immunocytochemistry

CEM cells were spun onto glass slides (Shandon, Cheshire, UK) or attached to poly-L-lysine-covered glass chamber slides (Labtek Naperville, IL), fixed and stained by immunocytochemistry for CD95 (clone DX2 from Chemicon, CA), ezrin (Biogenesis, UK), moesin (Transduction Laboratories, Lexington, KY) or tumor necrosis factor receptor 1 (Santa Cruz Biotechnology, CA), using the alkaline phosphatase anti-alkaline phosphatase (APAAP) (Dako, Denmark) method or the peroxidase-anti-peroxidase (PAP) (Dako) method, in single and double stainings, as appropriate (Fais *et al*., 1995).

Immunofluorescence

Control and treated cells were collected by centrifugation, attached to glass coverslips pre-coated with polylysine and fixed with 4% paraformaldehyde in phosphate-buffered saline (PBS) for 30 min at room temperature. After washing in the same buffer, cells were permeabilized with 0.5% Triton X-100 in PBS for 5 min at room temperature. For localization of CD95, ezrin, moesin and TNFR1 proteins, samples were incubated at 37°C for 30 min with polyclonal antibodies to CD95 (Santa Cruz Biotechnology) and tumor necrosis factor receptor 1 (Santa Cruz Biotechnology), or monoclonal antibodies to ezrin (Biogenesis, UK) and moesin (Transduction Laboratories). Cells were then incubated with anti-rabbit IgG FITC-conjugate (Sigma Chemical Co., St Louis, MO) or anti-mouse IgG TRITC-conjugate (Sigma) for detection of CD95 and ezrin proteins, respectively. After washing, all samples were mounted with glycerol-PBS (2:1) and observed with a Nikon Microphot fluorescence microscope. Double stainings were analyzed by IVM. Images were captured by a color chilled 3CCD camera (Hamamatsu, Japan). Normalization and background subtraction were performed for each image. Figures were obtained by adding CD95-FITC (green) and ezrin-TRITC (red) images by the OPTILAB (Graftek, France) software for image analysis.

PCR for ERM mRNAs

Total RNA was obtained by the RNAzol method. RNA templates were utilized for RT–PCR amplification. The primers used to detect the ERM mRNAs had the following sequences: 5′-CACGCTTGTCTTTAG-TGCTCC-3′ and 5′-ACTCAGACTTTACAGGCATTTTCC-3′ for ezrin (236 bp product); 5′-GCTAGGTGTTGATGCTTTGG-3′ and 5′-GAC-GTTCCATTAGCTCTTCC-3′ for radixin (420 bp product); 5′-TCCTAT-GGGAGTCAAGTGTGG-3′ and 5′-AGGTCCTGTCTCATTCCTAG-ACC-3′ for moesin (123 bp product). Primers used to amplify the GAPDH (195 bp product) were the following: 5′-CCATGGAGAAGG-CTGGGG-3′ and 5′-CAAAGTTGTCATGGATGACC-3′. The specificity of the sequences was verified by DDBJ/EMBL/GenBank Blast analysis. PCR products were analysed on a 1.5% agarose gel using ethidium bromide and UVB illumination for detection of DNA fragments.

Isolation and activation of peripheral blood lymphocytes

Human peripheral blood mononuclear cells (PBMC) were freshly isolated from healthy adult by layering on a Ficoll-Paque density gradient. Purified $CD3^+$ T cells were isolated from PBMCs by immunomagnetic negative selection using immunomagnetic beads coated with anti-CD14 and anti-CD20 mouse anti-human mAb (Dynal, Oslo, Norway). The resultant (unbound) T cell population contained >95% $CD3^+$ cells, as assessed by flow cytometric analysis. For T cell activation, purified T cells were incubated for 45 min at 4°C with the mAb anti-CD3 (purified by hybridoma cell line OKT3, the American Type Culture Rockville, IL) (Boirivant *et al*., 1996) at a concentration of 10 μg/ml. Antibody-bound

cells were then washed and crosslinked by incubation in 24-well Nuclon plates (Sigma) that had been previously coated with a goat anti-mouse Ab (BioSource, Camarillo, CA) (20 μg in carbonate buffer) and incubated for 6 days at 37°C (Algeciras-Schimnich *et al*., 1999). Alternatively, human PBL were activated with phytohemagglutinin (PHA) and IL-2, as described previously (Fais *et al*., 1999). At 1 and 6 days after activation cells were collected for flow cytometry, immunocytochemistry, immunofluorescence and immunoprecipitation.

Cell lysis and subcellular fractionation

CEM cells were pelleted and washed in cold PBS. Total cell extracts were obtained by solubilization in lysis buffer (AKT buffer) containing 20 mM Tris–HCl (pH 7.5), 150 or 500 mM NaCl (to avoid non-specific interactions), 10% glycerol, 1% NP-40 and both phosphatase and protease inhibitors (20 min, 4°C). Subcellular fractions from CEM cells, comprising cell membrane, cytoskeletal, cytosol and nuclear extracts were prepared as described previously (Bukrinskaya *et al*., 1998). Briefly, cells were pelleted, washed in PBS, resuspended in hypotonic solution (10 mM HEPES pH 6,9, 10 mM KCl, 3 μl/ml aprotinin, 0.1 mM PMSF) and incubated on ice for 15–20 min. Cells were disrupted by dounce homogenization (20 strokes). Nuclei were pelleted at 3200 r.p.m. for 3 min at 4°C and removed. Supernatant from pelleted nuclei was centrifuged further at 35 000 r.p.m. for 30 min at 4°C. The supernatant (cytosolic fraction) was separated and the pellet (cytoskeletal plus membrane fraction) was further resuspended in NTENT buffer (500 mM NaCl, 10 mM Tris–HCl pH 7.2, 1 mM EDTA, 3 μl/ml aprotinin, 0.1 mM PMSF, 1% Triton X-100). This fraction was directly immunoprecipitated with mAbs directed against Ezrin (Biogenesis, UK) or CD95 (clone DX2, Calbiochem) in the presence of protein A–Sepharose (Sigma). Alternatively the cytoskeletal plus membrane fraction was further centrifuged at 14000 r.p.m. for 30 min at 4°C. The resulting pellet, resuspended again in NTENT buffer, comprised the cytoskeletal fraction, while the supernatant comprised the membrane fraction.

Western blot analysis

Whole extracts and subcellular fractions were resuspended in SDS sample buffer, denaturated by boiling and separated on 10% SDS–PAGE gel. Proteins were then transferred to Hybond C Extra (Amersham) and blocked in 5% milk overnight. CD95, ezrin, moesin, CD4, actin and caspase-3 were detected with an anti-CD95 (clone 13, Transduction Laboratories), an anti-ezrin (Biogenesis), an anti-moesin (Transduction Laboratories), an anti-CD4 (Novocastra, Newcastle-upon-Tyne, UK) (Parolini *et al*., 1999), an anti-actin (Chemicon) and an anti-caspase-3 (Transduction Laboratories) mAb, respectively, and visualized with peroxidase anti-Ig followed by either ECL (Pierce, SuperSignal Substrate, IL) or the DAKO EnVision™ system, HRP and DAB as chromogen (DAKO), as appropriate.

Co-immunoprecipitation analysis

Cytoskeletal plus plasma membrane fraction obtained from CEM cells was pre-cleared with protein A–Sepharose 4B FastFlow (Sigma) (1 h, 4°C). CD95 protein was immunoprecipitated from pre-cleared lysate with anti-CD95 antibodies (clone DX2, Calbiochem) overnight at 4°C in the presence of protein A–Sepharose. Alternatively, ezrin or moesin protein were immunoprecipitated as described above for CD95, using an anti-ezrin mAb (Biogenesis) or an anti-moesin mAb (Transduction Laboratories). Immunoprecipitated beads were washed four times in NTENT buffer, resuspended in SDS sample buffer and resolved in 10% SDS–PAGE gel. Then, proteins were transferred to nitrocellulose membrane and analyzed by western blotting with an anti-ezrin mAb (Biogenesis), an anti-moesin mAb (Transduction Laboratories) or an anti-CD95 mAb (clone 13, Transduction Laboratories), as appropriate. The immunoblotting for CD95 in ezrin or moesin immunoprecipitates (Transduction Laboratories) was performed resuspending the immunoprecipitates in Laemmli buffer (Laemmli, 1970), before SDS–PAGE, to avoid the usual migration of immunoglobulin heavy chains close to the CD95 molecular weight. The control experiment was performed only using immunoprecipitating antibodies (anti-ezrin or anti-CD95 as appropriate) in NTENT buffer to exclude heavy chain cross-reactivity of the secondary antibody. Pre-stained standards not containing β-mercaptoethanol (Rainbow™ colored protein molecular weight markers, Amersham UK) were used for experiments performed with Laemmli buffer.

Antisense oligonucleotides

Two antisense phosphorothioate oligonucleotides (S-modified) complementary to the corresponding position 196–217 of the human ezrin and to the corresponding position 1–15 of the human moesin coding regions, respectively, were used. The chosen sequence was AGACGGGTC-CTCCAGTCCTTC for the ezrin antisense, and TACGGGTTTTGCTAG for the moesin antisense. The PONs were synthesized by Amersham Europe (Freiburg, Germany). The oligonucleotides were suspended in serum-free medium and added into the culture medium every 12 h at a concentration of 40 μM for 96 h. Every 24 h CEM cells were washed and re-suspended in fresh medium containing 40 μM PONs. Sense PONs of the same region, pre-treatment and non-treatment, were used as controls.

Flow cytometry

Three-color cytofluorimetric analysis of day 1- and day 6-activated PBMC was performed. Cells (5×10^5) were incubated for 10 min in PBS 10% AB human serum. After this time cells were incubated at 4°C with saturating concentration of directly conjugated: (i) FITC-anti-CD69, PE-anti-CD95 (MBL International Corporation, Watertown, USA) PerCP-anti-CD4; (ii) FITC-anti-CD45RO, PE-anti-CD95, PerCP-anti-CD4; and (iii) isotype matched normal FITC, PE and PerCP Ab (Becton Dickinson, Mountain View, CA). Cells were then washed twice in cold PBS/azide and resuspended for three-color cytofluorimetric analysis. For the acquisition of samples, FL1/FL2 compensation was 1.4%, FL2/FL1 compensation was 40.5%, FL2/FL3 compensation was 4.0%, and FL3/FL2 compensation was 36.0%. A minimum of 30 000 events per sample were acquired. Relative fluorescent intensity of individual cells were recorded and statistically analyzed on a Macintosh computer using CellQuest Software. Statistical analysis was performed by the parametric Kolmogorov–Smirnov (K/S) test.

For cytofluorimetric evaluation of apoptosis of untreated and CD95, triggered CEM cells (125 ng/ml of IgM anti-CD95 antibody) or PBMC (500 ng/ml of IgM anti-CD95 antibody) were washed and double stained by using annexin V–fluorescein isothiocyanate (FITC) apoptosis detection kit (Eppendorf, Milan, Italy). Cells that have lost membrane integrity (therefore considered as necrotic cells) will show red staining [propidium iodide (PI) (Molecular Probes, Eugene, OR)] throughout the nucleus and will be easily distinguishable from living cells. After 10 min incubation in the dark with annexin V–FITC and PI (40 μg/ml), samples were washed and immediately analyzed on a FACScan flow cytometer (Becton Dickinson) equipped with a 488 nm argon laser. At least 20 000 events have been acquired. Data were recorded and statistically analyzed (Student's *t*-test) on a Hewlett Packard computer using the Lysys II Software.

Cytochalasin D

Control and treated cells were exposed to cytochalasin D (CD, Sigma Chemical Co.) before different apoptotic inducers. The CD dose used in this study (0.5 μg/ml) inhibits actin polimerization without being cytotoxic, as assessed by analytical cytology analyses (Cooper, 1987).

Induction of apoptosis

Anti-human CD95 treatment. An anti-human IgM mAb (125 ng/ml) (clone CH11, Upstate Biotechnology, Lake Placid, NY) was added to CEM cell cultures (6×10^5 cells/ml). After overnight treatment, cells were collected, washed and analyzed for apoptosis.

TNFα treatment. CEM cells (6×10^5/ml) were treated with 50 IU/ml TNFα (Sigma Chemical Co.) as described previously (Conti *et al*., 1998).

UVB radiation. Cells (6×10^5 per ml) were exposed to UVB irradiation in PBS using a Philips TL 20 W/12 lamp localized in a sterile wood. In order to eliminate UVC radiation, a Kodak filter (Kodacell TL 401) with an optical density of <0.4 for wavelengths below 285 nm was employed and was placed on Petri dishes during exposure. In these conditions, the UVB radiant flux density to the cells was 2.2 W/m^2, as verified by an Osram centra UV meter. Twenty-four hours after UVB irradiation, control and treated cells were prepared for fluorescence and scanning electron microscopy (Malorni *et al*., 1994).

Staurosporine treatment. The protein kinase inhibitor staurosporin (Sigma, 1000× stock in dimethylsulfoxide) was added to the culture medium at a final concentration of 30 nM (Eischen *et al*., 1997). After 24 h treatment, control and treated cells were prepared for fluorescence and SEM.

Evaluation of apoptotic cells

Quantitative evaluation of apoptotic cell death was performed by flow cytometry and/or static cytometry using the chromatin dye Hoechst 33258 (Molecular Probes) as described previously (Malorni *et al*., 1993b). The numbers reported were the mean values ± SD for five independent experiments.

Acknowledgements

We are grateful to Drs Ruggero De Maria, Ugo Testa, Giovina Ruberti and Marco Tripodi for helpful discussion. This work was supported in part by grants from the Italian Ministry of Health (40C/F and 30C/I, III National Research Program on AIDS) and by the Coordinated Grant 'Identification of the new human tumor antigens and strategies to enhance their immunogenicity and override tumor escape' from the Associazione Italiana per la Ricerca sul Cancro (Milan, Italy).

References

Alderson,M.R. *et al*. (1995) Fas ligand mediates activation induced cell death in human T lymphocytes. *J. Exp. Med.*, **181**, 71–77.

Algeciras-Schimnich,A., Griffith,T.S., Lynch,D.H., and Paya,C.V. (1999) Cell cycle-dependent regulation of FLIP levels and susceptibility to Fas-mediated apoptosis. *J. Immunol.*, **162**, 5205–5211.

Apoptosis (special section) (1998) *Science*, **281**, 1241–1404.

Boirivant,M., Pica,R., DeMaria,R., Testi,R., Pallone,F., and Strober,W. (1996) Stimulated human lamina propria T cells manifest enhanced Fas-mediated apoptosis. *J. Clin. Invest.*, **98**, 2616–2622.

Bretscher,A. (1999) Regulation of cortical structure by ezrin-radixin-moesin protein family. *Curr. Opin. Cell Biol.*, **11**, 109–116.

Brunner,T. *et al*. (1995) Cell-autonomous Fas (CD95)/Fas ligand interaction mediates activaction induced apoptosis in T-cell hybridomas. *Nature*, **373**, 441–444.

Bukrinskaya,A., Brichacek,B., Mann,A. and Stevenson,M. (1998) Establishment of a functional human immunodeficiency virus type 1 (HIV-1) reverse transcription complex involves the cytoskeleton. *J. Exp. Med.*, **188**, 2113–2125.

Cao,T.T., Deacon,H.W., Reczek,D., Bretscher,A. and von Zastrow,M. (1999) A Kinase-regulated PDZ-domain interaction controls endocytic sorting of the β2-adrenergic receptor. *Nature*, **401**, 286–289.

Clarke,E.A., and Brugge,J.S. (1995) Integrins and signal transduction pathway: the road taken. *Science*, **268**, 233–239.

Conti,L. *et al.* (1998) The HIV-1 vpr protein acts as a negative regulator of apoptosis in a human lymphoblastoid T cell line: a possible implication for the pathogenesis of AIDS. *J. Exp. Med.*, **187**, 403–413.

Cooper,J.A. (1987) Effects of cytochalasin and phalloidin on actin. *J. Cell Biol.*, **105**, 1473–1478.

Defacque,H. *et al.* (2000) Involvement of ezrin/moesin in *de novo* actin assembly on phagosomal membranes. *EMBO J.*, **19**, 199–212.

del Pozo,M.A., Sanchez-Mateos,P. and Sanchez-Madrid,F. (1996) Cellular polarization induced by chemokines: a mechanism for leukocyte recruitment? *Immunol. Today*, **17**, 127–131.

del Pozo,M.A., Cabanas,C., Montoya,M.C., Ager,A., Sanchez-Mateos,P. and Sanchez-Madrid,F. (1997) ICAMs redistributed by chemokines to cellular uropods as a mechanism for recruitment of T lymphocytes. *J. Cell Biol.*, **137**, 493–508.

De Maria,R., Boirivant,M., Cifone,M.G., Roncaioli,P., Hahne,M., Tschopp,J., Pallone,F., Santoni,A. and Testi,R. (1996) Functional expression of Fas and Fas ligand on human gut lamina propria T lymphocytes. A potential role for the acidic sphingomyelinase pathway in normal immunoregulation. *J. Clin. Invest.*, **97**, 316–322.

Dransfield,D.T., Bradford,A.J., Smith,J., Martin,M., Roy,C., Mangeat,P. and Goldenring,J.R. (1997) Ezrin is a cyclic AMP-dependent protein kinase anchoring protein. *EMBO J.*, **16**, 35–43.

Drubin,D.G. and Nelson,W.J. (1996) Origins of cell polarity. *Cell*, **84**, 335–344.

Eischen,C.M., Kottke,T.J., Martins,L.M., Basi,G.S., Tung,J.S., Earnshaw,W.C., Leibson,P.J. and Kaufmann,S.H. (1997) Comparison of apoptosis in wild-type and Fas-resistant cells: chemotherapy-induced apoptosis is not dependent on Fas/Fas ligand interactions. *Blood*, **90**, 935–943.

Fais,S., Burgio,V.L., Silvestri,M., Capobianchi,M.R., Pacchiarotti,A. and Pallone,F. (1994) Multinucleated Giant Cells (MGC) generation induced by interferon gamma. Changes in the expression and distribution of the intercellular adhesion molecule-1 (ICAM-1) during macrophages fusion and MGC formation. *Lab. Invest.*, **71**, 737–744.

Fais,S., Capobianchi,M.R., Abbate,I., Castilletti,C., Gentile,M., Cordiali Fei,P., Ameglio,F. and Dianzani,F. (1995) Unidirectional budding of HIV-1 at the site of cell-to-cell contact is associated with co-polarization of intercellular adhesion molecule-1 and HIV-1 viral matrix protein. *AIDS*, **9**, 329–335.

Fais,S., Burgio,V.L., Capobianchi,M.R., Gessani,S., Pallone,F. and Belardelli,F. (1997) The biological relevance of polycaryons in the immune response. *Immunol. Today*, **18**, 522–527.

Fais,S., Lapenta,C., Santini,S.M., Spada,M., Parlato,S., Logozzi,M., Rizza,P. and Belardelli,F. (1999) R5 and X4 HIV-1 strains induce different pathogenic effects in hu-pbl-scid mice depending on the state of activation/differentiation of human target cells at the time of primary infection. *J. Virol.*, **73**, 6453–6459.

Geiger,B., Rosen,D. and Berke,G.J. (1982) Spatial relationships of microtubule-organizing centers and the contact area of cytotoxic T lymphocytes and target cells. *J. Cell Biol.*, **95**, 137–143.

Giordano,C. *et al.* (1997) Potential involvement of Fas and its ligand in the pathogenesis of Hashimoto's thyroiditis. *Science*, **275**, 960–963.

Heiska,L., Alfthan,K., Gronholm,M., Vilja,P., Vaheri,A. and Carpen,O. (1998) Association of ezrin with intercellular adhesion molecule-1 and -2 (ICAM-1 and ICAM-2). Regulation by phosphatidylinositol 4, 5-biphosphate. *J. Biol. Chem.*, **273**, 21893–21900.

Klas,C., Debatin,K.M., Jonker,R.R. and Krammer,P.H. (1993) Activation interferes with the APO-1 pathway in mature human T cells. *Int. Immunol.*, **5**, 625–630.

Kupfer,H., Swain,S.L.,Jr, Janeway,C.A. and Singer,S.J. (1986) The specific direct interaction of helper T-cells and antigen presenting B cells. *Proc. Natl Acad. Sci. USA*, **83**, 6080–6083.

Kupfer,H., Monks,C.R.F. and Kupfer,A. (1994) Small splenic B cells that bind to antigen-specific T helper (Th) cells and face the site of cytokine production in the Th cells selectively proliferate: immunofluorescence microscopic studies of Th-B antigen-presenting cell interactions. *J. Exp. Med.*, **179**, 1507–1515.

Kusumi,A. and Sako,Y. (1996) Cell surface organization by the membrane skeleton. *Curr. Opin. Cell Biol.*, **8**, 566–574.

Laemmli,U.K. (1970) Cleavage of structural proteins during the assembly of the head of bacteriophage T4. *Nature*, **227**, 680–685.

Larrick,J.W. and Wright,S.C. (1990) Cytotoxic mechanism of tumor necrosis factor α. *FASEB J.*, **4**, 3215–3223.

Linch,D.H., Ramsdell,F. and Alderson,M.R. (1995) Fas and FasL in the homeostatic regulation of immune responses. *Immunol. Today*, **16**, 569–574.

Luna,E.J. and Hitt,A.L. (1992) Cytoskeleton-plasma membrane interactions. *Science*, **258**, 955–963.

Malorni,W., Iosi,F., Santini,M.T. and Testa,U. (1993a) Menadione-induced oxidative stress leads to a rapid down modulation of transferrin receptor recycling. *J. Cell Sci.*, **106**, 309–318.

Malorni,W., Rivabene,R., Santini,M.T. and Donelli,G. (1993b) *N*-acetylcysteine inhibits apoptosis and decreases viral particles in HIV-chronically infected U937 cells. *FEBS Lett.*, **327**, 75–78.

Malorni,W., Donelli,G., Straface,E., Santini,M.T., Paradisi,S. and Giacomoni,P.U. (1994) Both UVA and UVB induce cytoskeleton-dependent surface blebbing in epidermoid cells. *J. Photochem. Photobiol. B.*, **26**, 265–270.

Mangeat,P., Roy,C. and Martin,M. (1999) ERM proteins in cell adhesion and membrane dynamics. *Trends Cell Biol.*, **9**, 187–192.

Maniotis,A.J., Chen,C.S. and Ingber,D.E. (1997) Demonstration of mechanical connection between integrins, cytoskeletal filaments, and nucleoplasm that stabilize nuclear structure. *Proc. Natl Acad. Sci. USA*, **94**, 849–854.

Mehlen,P., Kretz-Remy,C., Briolay,J., Fostan,P., Mirault,M. and Arrigo,A. (1995) Intracellular reactive oxygen species as apparent modulators of heat-shock protein 27 (hsp27) structural organization and phosphorylation in basal and tumor necrosis factor α–treated T47D human carcinoma cells. *Biochem. J.*, **312**, 367–375.

Miyawaki,T., Uehara,T., Nibu,R., Tsuji,T., Yachie,A., Yonehara,S. and Taniguchi,N. (1992) Differential expression of apoptosis-related Fas antigen on lymphocyte subpopulations in human peripheral blood. *J. Immunol.*, **149**, 3753–3758.

Nagata,S. (1997) Apoptosis by death factor. *Cell*, **88**, 335–365.

Nagata,S. and Suda,T. (1995) Fas and Fas ligand: lpr and gld mutations. *Immunol. Today*, **16**, 39–43.

Nelson,W.J. (1992) Regulation of cell surface polarity from bacteria to mammals. *Science*, **258**, 948–955.

Parolini,I. *et al*. (1999) Phorbol ester-induced disruption of the CD4-Lck complex occurs within a detergent-resistant microdomain of the plasma membrane. *J. Biol. Chem.*, **274**, 14176–14187.

Peter,M.E. and Krammer,P.H. (1998) Mechanism of CD95 (APO-1/Fas)-mediated apoptosis. *Curr. Opin. Immunol.*, **10**, 545–551.

Serrador,J.M., Alonso-Lebrero,J.L., Del Pozo,M.A., Furthmayr,H., Schwartz-Albiez,R., Calvo,J., Lozano,F. and Sanchez-Madrid,F. (1997) Moesin interacts with the cytoplasmic region of intercellular

adhesion molecule-3 and is redistribuited to the uropod of T lymphocytes during cell polarization. *J. Cell Biol.*, **138**, 1409–1423.
Serrador,J.M. *et al.* (1998) CD43 interacts with moesin and ezrin and regulates its redistribution to the uropods of T lymphocytes at the cell-cell contacts. *Blood*, **91**, 4632–4644.
Shcherbina,A., Bretscher,A., Kenney,D.M. and Remold-O'Donnel,E. (1999) Moesin, the major ERM protein of lymphocytes and platelets, differ from ezrin in its insensitivity to calpain. *FEBS Lett.*, **443**, 31–36.
Stowers,L., Yelon,D., Berg,L.J. and Chant,J. (1995) Regulation of the polarization of T cells toward antigen-presenting cells by Ras-related GTPase CDC42. *Proc. Natl Acad. Sci. USA*, **92**, 5027–5031.
Suda,T., Hashimoto,H., Tanaka,M., Ochi,T. and Nagata,S. (1997) Membrane Fas ligand kills human peripheral blood T lymphocytes and soluble fas ligand blocks the killing. *J. Exp. Med.*, **186**, 2045–2050.
Tschopp,J., Irmler,M. and Thome,M. (1998) Inhibition of Fas death signals by FLIPs. *Curr. Opin. Immunol.*, **10**, 552–558.
Tsukita,S., Oishi,K., Sato,N., Sagara,J., Kawaki,A. and Tsukita,S. (1994) ERM family members as molecular linkers between the cell surface glycoprotein CD44 and actin-based cytoskeletons. *J. Cell Biol.*, **126**, 391–401.
Tsukita,S., Yonemura,S. and Tsukita,S. (1997) ERM (ezrin/radixin/moesin) family: from cytoskeleton to signal transduction. *Curr. Opin. Cell Biol.*, **9**, 70–75.
Wallach,D., Varfolomeev,E.E., Malinin,N.L., Goltsev,Y.V., Kovalenko, A.V. and Boldin,M.P. (1999) Tumor necrosis factor receptor and Fas signaling mechanisms. *Annu. Rev. Immunol.*, **17**, 331–367.
Yamada,K.M. and Geiger,B. (1997) Molecular interactions in cell adhesion complexes. *Curr. Opin. Cell Biol.*, **9**, 76–85.
Yonemura,S., Hirao,M., Yoshinori,D., Takahashi,N., Kondo,T., Tsukita,S. and Tsukita,S. (1998) Ezrin/radixin/moesin (ERM) proteins bind to positively charged amino acid cluster in the juxta-membrane cytoplasmic domain of CD44, CD43 and ICAM-2. *J. Cell Biol.*, **140**, 885–895.

Received April 10, 2000; revised August 1, 2000;
accepted August 15, 2000